

Ultrasound Localization of Sub-Wavelength Surgical Guidewires in Support of Prolonged Field Care

Linda J. Olafsen, Ph.D.¹, **Daniella R DeVries, M.S.¹**, Maxwell Salter¹, Hahn Nguyen, M.S.¹, Jeffrey S. Olafsen, Ph.D.¹, Keith E. Schubert, Ph.D.¹, Daniel C. Lee, M.D.^{2,3}, Samantha Dayawansa, M.D., Ph.D.⁴, Jason H. Huang, M.D.^{4,5}



Background

The ability to effectively insert and guide surgical tools through an artery to the brain for neurological monitoring, wound embolization, and other treatments offers significant potential enhancement of prolonged field care efforts in combat support hospitals. Currently, minimally invasive aneurysm repair surgeries are performed using stiff guide wires to allow surgeons to navigate to the affected areas via the arterial network of the body using X-ray fluoroscopy to locate the position of the wire. This use of radiative imaging exposes all surgical staff to radiation each time the procedure is performed. The goal is to create a navigation package that addresses three main areas:

1. Improve guide wire using shape memory alloy to allow for a moveable guide wire
2. Implement a non-radiative imaging technique
3. Integrate sensors for navigation and vitals monitoring

Objectives

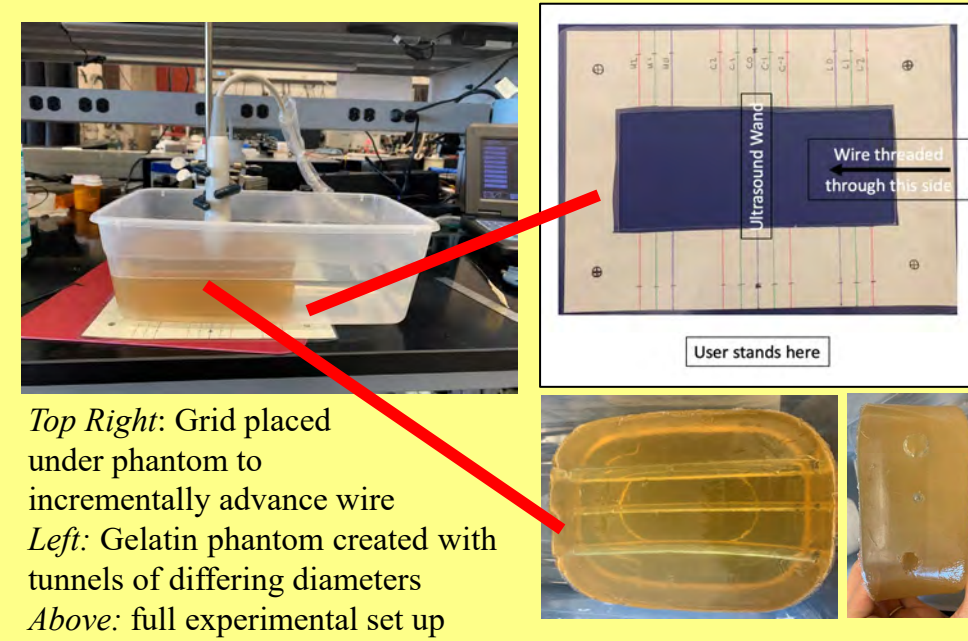
- Improved navigation and reduced time to reach treatment site
- Delivering imaging devices for intravenous optical tumor monitoring and optical sensing of oxygenation levels with greater correlation and specificity
- Increased sensitivity to biomarkers due to reduced optical path of in vivo sensors
- Future capability to automate/remotely control treatment in remote locations such as combat support hospitals, utilizing telemedicine
- Revolutionizing minimally invasive surgery, including spinal surgery

Benefits to the Warfighter

- Embolization and remote neurological surgery for stabilization pending transfer to definitive care hospital
- Remote control for health care consultation and early diagnosis
- Ultrasound imaging modality supports implementation at combat support hospitals because of greater mobility and less expense

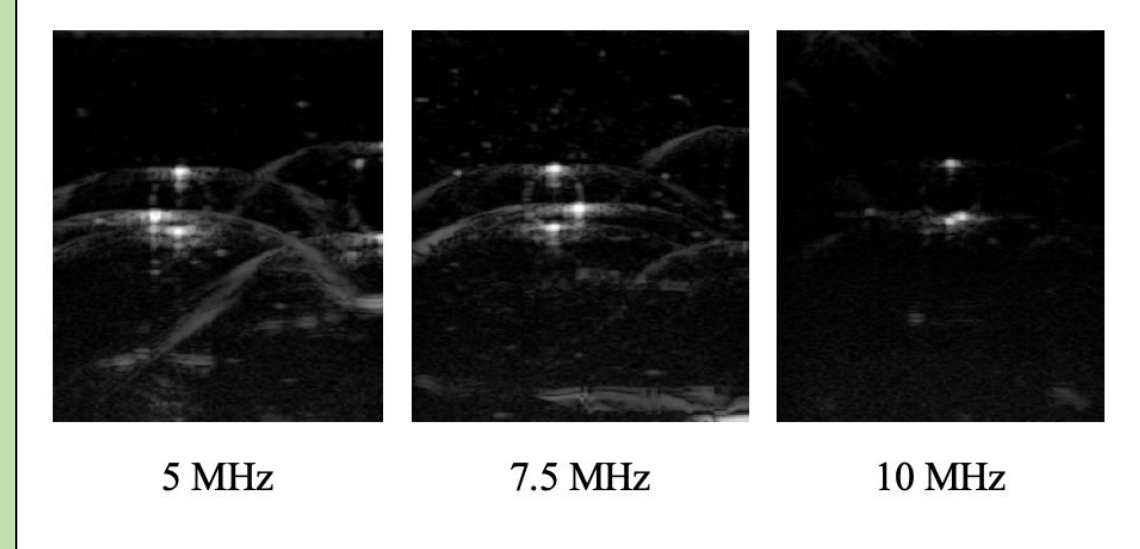
Method

- Rectangular gelatin phantoms created for modeling tissue for ultrasound imaging
 - Different diameter tunnels through lengthwise to mimic vessels
- Ultrasound probe is held at the center at position C0 on the grid (top right) while the tip of the wire is incrementally advanced
- Ultrasound images are taken at position C0 to show the progress of the wire through the phantom
- Imaging was done for four diameter tunnels (1/4", 3/8", 1/2", 5/8"), six wire diameters (50, 75, 100, 125, 150, 250 μ m), and three ultrasound operating frequencies (5, 7.5, 10 MHz)

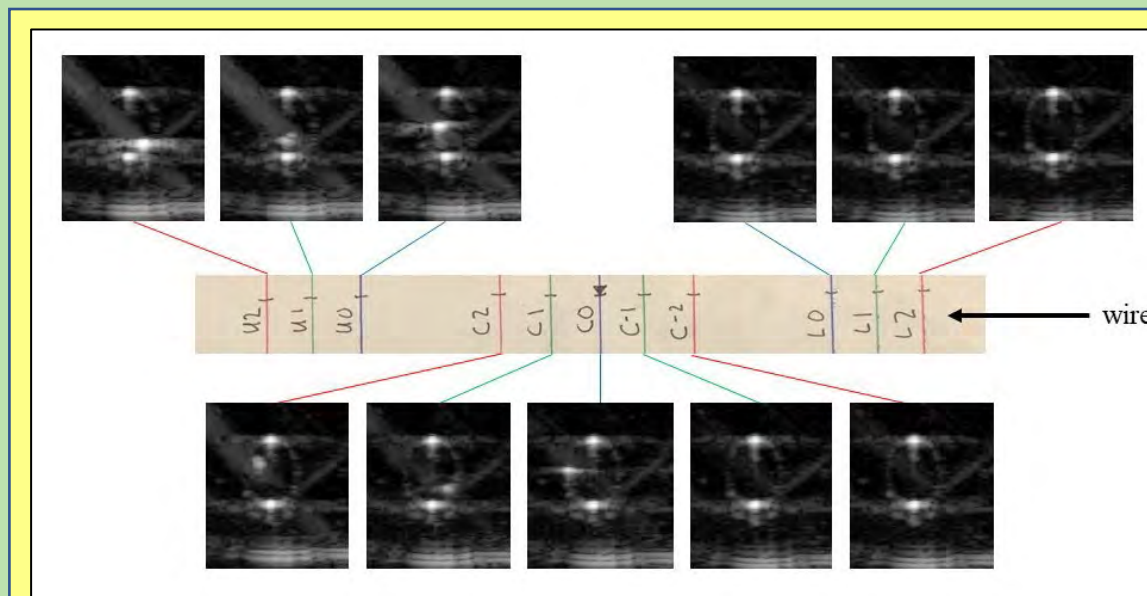


Results

Ultrasound produces black and white images based on the strength of the reflected wave that it produces. The color gradient is dependent on the density of the object it passes through. The current ultrasound machine operates at frequencies between 5 and 10 MHz. The 10 MHz range produces a wavelength of 154 μ m. We can locate wires smaller than this via ultrasound through reflections, but images produced are not images of the wire directly. Below is 100 μ m wire imaged at the U2 position.

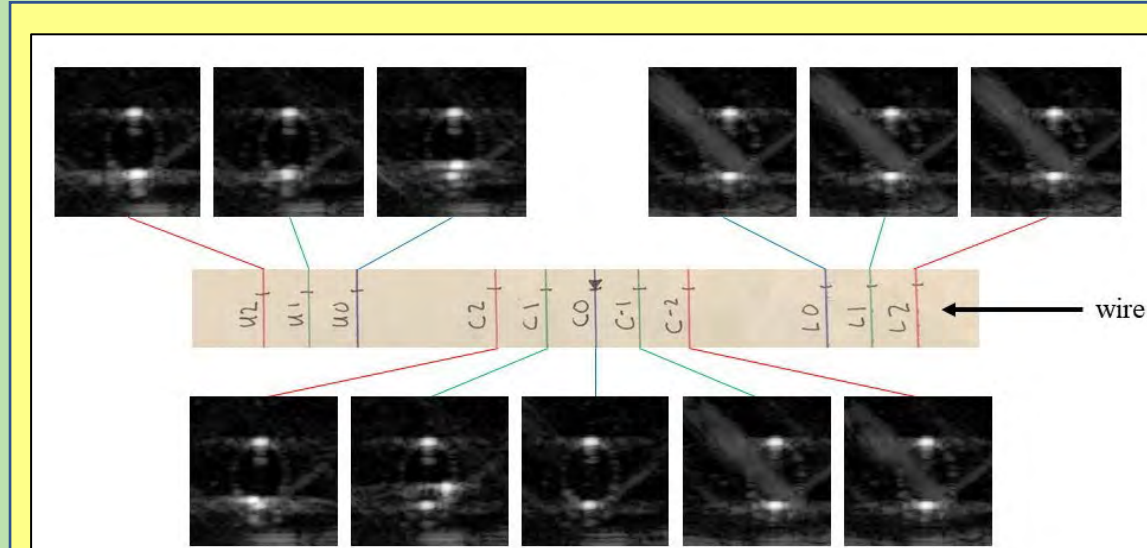


5 MHz produces the brightest spot for the wire but with the most noise. 10 MHz produces the least noise but dimmest spot. 7.5 MHz is in between and offers the best images for visual inspection and locating of the wire.



75 μ m wire in 1/4" diameter tunnel imaged at 7.5 MHz

The 50 μ m (below) and 75 μ m (above) wires were imaged as in the described Method section. Each image is taken from position C0 while the grid location denotes the advancement of the tip of the wire.



50 μ m wire in 1/4" diameter tunnel imaged at 7.5 MHz

Difference Imaging

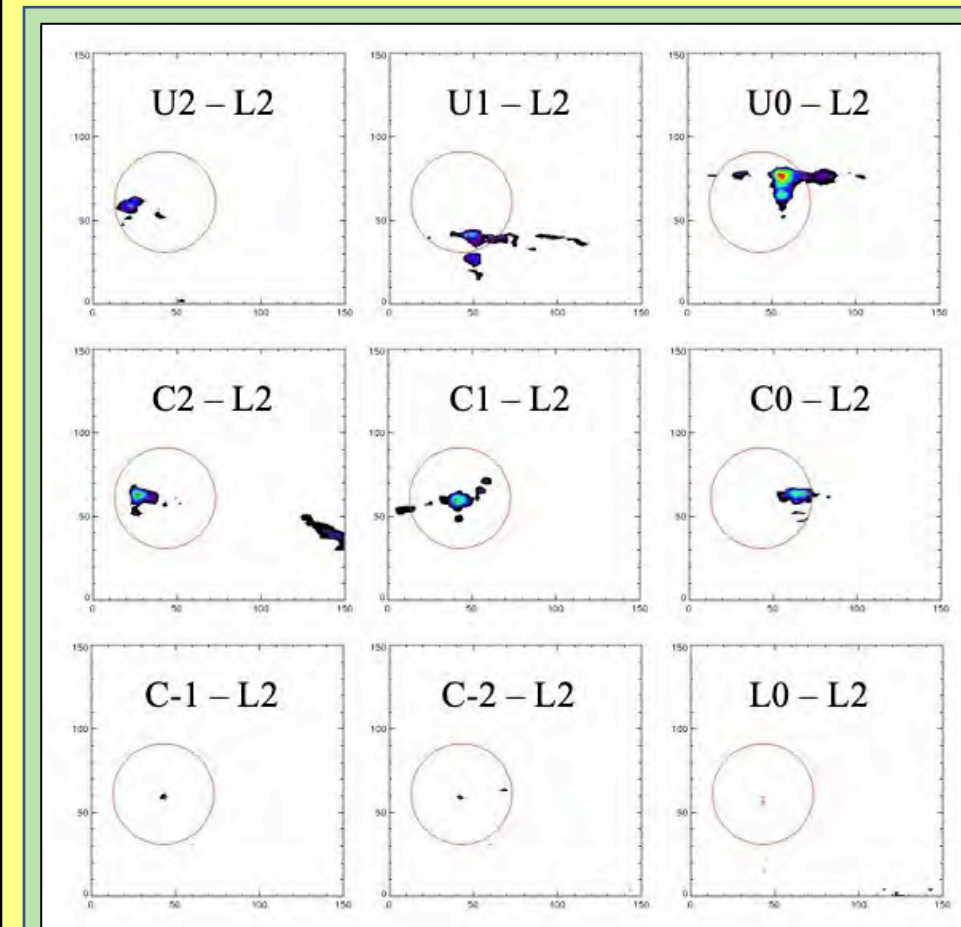
Difference images of the 75 μ m wire at 5 MHz were made subtracting the image at position L2 from all other positions because this is where the tip of the wire is farthest from the ultrasound probe, thus the least likely to produce a signal. 5 MHz was chosen for the best signal strength and the amount of noise was less important due to subtracting images.

- Signal can be seen much earlier than with visual inspection
- Evidenced by the bottom three images, where the wire has not yet passed under the probe, where small amounts of signal is seen within the red ring (left, top)
- Pixel intensities of the difference images as surface plots to see the data in a three-dimensional format (left, bottom)

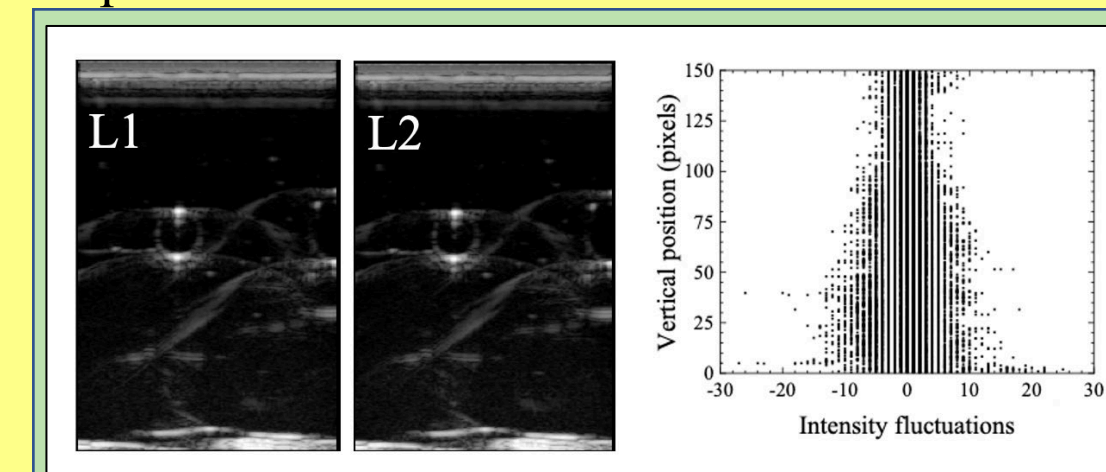
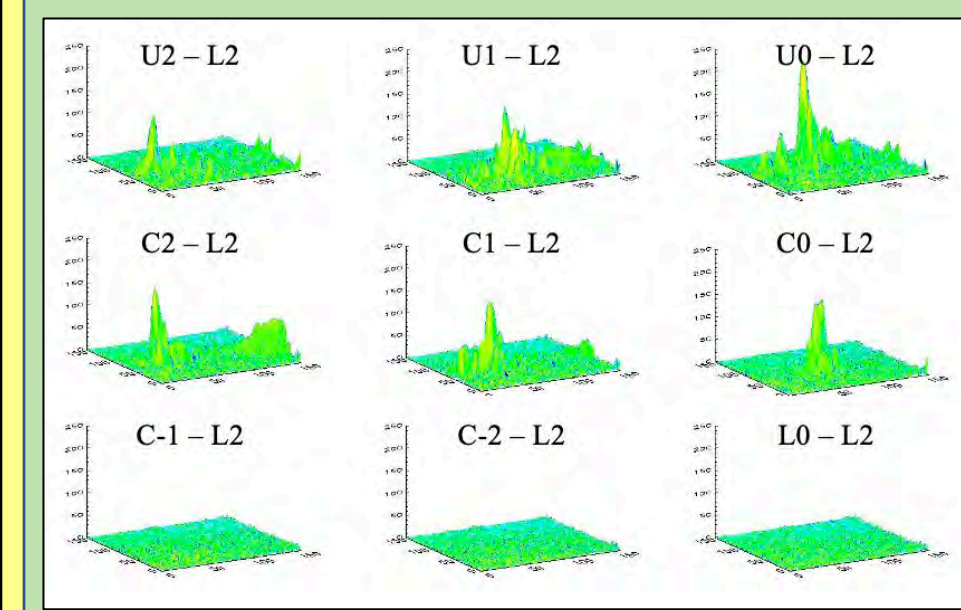
Background noise fluctuation was analyzed with the L1 and L2 images because they are the farthest from the ultrasound probe, thus the least likely to see signal from the wire itself (right, top).

- As depth increases, noise increases
- Peak pixel intensity vs. position shows quantitative confirmation of wire visibility from positions C0 to U2 (right, bottom right)
- Yields signal to noise ratio of 8.7

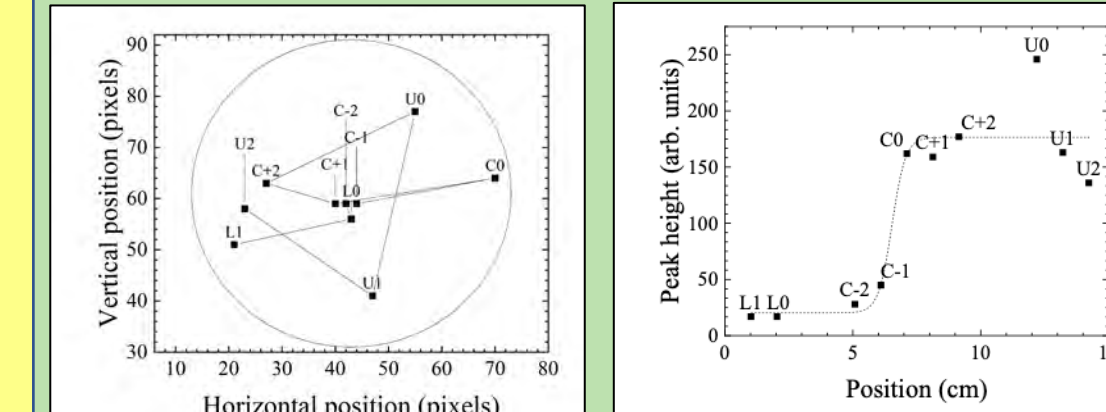
This peak pixel intensity is them plotted in terms of position within the tunnel. The circle represents the boundaries of the tunnel. It creates a clockwise corkscrew shape as it progresses which is to be expected due to wires initially being dispensed on a spool.



Above: Difference images of 75 μ m wire at 5 MHz
Below: Pixel intensity surface plots of above difference images



Above: Background noise fluctuation analysis with raw images used
Below Left: Peak pixel intensity location plot for 75 μ m wire at 5 MHz
Below Right: Peak pixel intensity for 75 μ m at 5 MHz

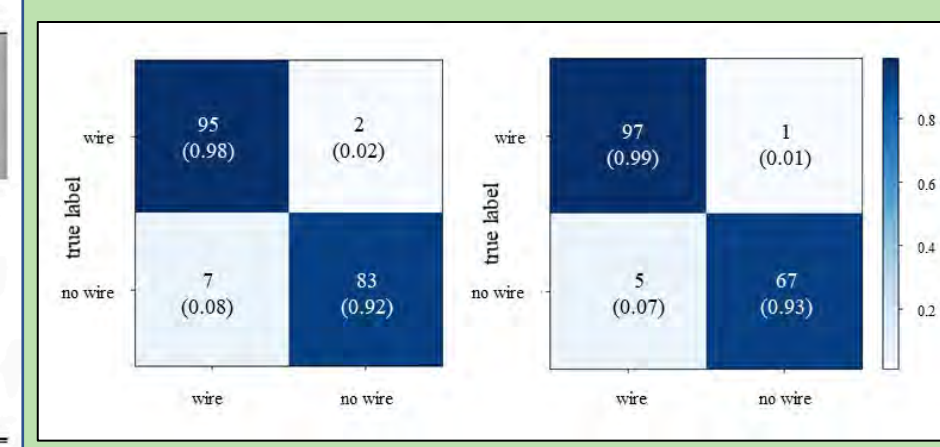


Convolution Neural Network (CNN)

CNNs are one of the most popular types of deep learning, a subset of machine learning that uses a neural network multilayer neural networks to perform desired tasks by using training models. VGG-16 is a pretrained CNN model, developed by Simonyan and Zisserman of the Visual Geometry Group from the University of Oxford, executed to classify the ultrasound images with and without the Nitinol wire. Each of the two data sets, the original ultrasound images and the difference images, are split into a training set and validation set. After importing the VGG-16 model, the three fully connected layers are discarded. The new specialized CNNs are then trained using the data sets. A regular sigmoid function is used to classify the images into two classes of with and without the wire. The newly trained specialized CNN is fed the features from the frozen VGG-16 model and the pre-trained weights are loaded into the model. Results obtained from application of the CNN are shown below.

	REGULAR IMAGES	95% CI	DIFFERENCE IMAGES	95% CI
True Positive	95		97	
False Positive	2		1	
False Negative	7		5	
True Negative	83		67	
Accuracy	95.19%	0.9106-0.9778	96.47%	0.9248-0.9869
Sensitivity	93.14%	0.8823-0.9814	95.10%	0.90908-0.99288
Specificity	97.94%	0.9511-1.00766	98.53%	0.95668-1.0139
Positive Prediction Value	97.94%	0.9511-1.00766	98.98%	0.9699-1.00969
Negative Prediction Value	92.22%	0.86689-0.97755	93.06%	0.87184-0.98927

Confusion Matrices



Future Work

- Inclusion of infrared wire tip sensors for monitoring oxygenation and aid in wire imaging
- Development of smaller, more efficient infrared emitters for deeper penetration
- Development of improved gelatin phantoms that can be optically tuned for testing of infrared sensors
- Create a blood phantom to mimic particle suspension in fluid, oxygenation levels, and scattering

Advantages

- Treatment of aneurysms
- Clot-breaking devices for treating strokes
- Camera/detector attachment for endovascular in vivo sensing and imaging
- Greater portability with less expense
- Enhanced endovascular navigation to treatment sites
- Future opportunities for telemedicine and remote intervention by specialists

Institutional Affiliations

- 1 Baylor University, Waco, TX
- 2 Anne Arundel Health System, Annapolis, MD
- 3 Johns Hopkins University School of Medicine, Baltimore, MD
- 4 Baylor Scott & White Health Neuroscience Institute, Temple, TX
- 5 Texas A&M University College of Medicine, Temple, TX

References

- [1] L. J. Olafsen, B. Jones, L. Sparks, H. H. Nguyen, A. Tanner, K. E. Schubert, J. S. Olafsen, S. Dayawansa, E. Fonkem, and J. H. Huang, "Current-controlled Nitinol wire for improved arterial navigation," *Proceedings of the SPIE* **10868**, 108681E (2019).
- [2] S. Dayawansa, D. R. DeVries, L. J. Olafsen, K. E. Schubert, J. S. Olafsen, and J. H. Huang, 2021 Congress of Neurological Surgeons Annual Meeting (16–20 October 2021, Austin, TX), "Ultrasound (US) scans to substitute X-ray devices during endovascular procedures" (poster).
- [3] S. Dayawansa, E. A. Benardete, P. T. Noonan, L. J. Olafsen, J. S. Olafsen, K. E. Schubert, and J. H. Huang, "Optimum wide neck bifurcation aneurysm angle change (BSW index) promotes better coiling of the aneurysm," 2018 American Association of Neurological Surgeons Annual Scientific Meeting.
- [4] K. Simonyan and A. Zisserman, "Very deep convolutional networks for large-scale image recognition," 2015. <https://arxiv.org/abs/1409.1556>